Heat capacity and turbidity near the critical point of succinonitrile–water

A. W. Nowicki, Madhujit Ghosh, S. M. McClellan, and D. T. Jacobs[a)]
Physics Department, The College of Wooster, Wooster, Ohio 44691

(Received 23 October 2000; accepted 7 December 2000)

Both the heat capacity and the turbidity of the liquid–liquid mixture succinonitrile–water near its upper critical consolute point were measured and two amplitude relations were tested. Using an adiabatic calorimeter to measure the heat capacity and the transmitted light intensity to determine the turbidity, precise and reproducible data determined the critical exponents α, ν, and γ consistent with theoretical predictions. The correlation length $\xi_0 = 0.168 \pm 0.004$ nm was determined from the turbidity experiment while the heat capacity amplitudes were $A^+ = 0.0543 \pm 0.0004$ J/(cm^3 K) in the one- and $A^- = 0.1013 \pm 0.0004$ J/(cm^3 K) in the two-phase region. The amplitude ratio $A^+/A^- = 0.536 \pm 0.005$ was consistent with other experimental determinations in liquid–liquid mixtures or liquid–vapor systems, and with recent theoretical predictions. The two-scale-factor universality ratio X, now consistent among experiments and theories with a value between 0.017 and 0.020, was determined to be 0.0187 ± 0.0013. © *2001 American Institute of Physics.*
[DOI: 10.1063/1.1344613]

I. INTRODUCTION

Critical point phenomena encompasses both simple and complex systems near a critical point as well as over an extended region in thermodynamic space. Large density or concentration fluctuations near a system's critical point effectively mask the identity of the system and produce universal phenomena which have been well studied in simple liquid–vapor and liquid–liquid systems.[1–3] Such systems have provided useful model systems to test theoretical predictions which can then be extended to more complicated systems. Several quantities exhibit a simple power-law dependence close to the critical point, which are described by universal exponents. Liquid–liquid mixtures, liquid–vapor systems, and uniaxial ferromagnetic materials belong[1–3] to the three-dimensional Ising model which, in a renormalization group (RG) context, predicts[4] values for the critical exponents that agree with experimental results.[1–3] Several universal amplitude ratios have also been predicted and many have been experimentally tested with mixed results.[5] A particularly powerful observation is that only two critical exponents are linearly independent, and that the leading amplitudes can be interrelated using only two scale factors.[1–3] Thus, the amplitudes from two experiments could determine all the leading critical behavior of a given system.

The heat capacity provides a delicate probe of the system near a critical point and can determine essential amplitude and exponent values. In particular, a precise measurement of the heat capacity of the liquid–liquid mixture succinonitrile–water at its critical composition will determine the amplitudes of the power-law divergence in the one- and two-phase regions and their ratio, which is predicted to be universal. An independent turbidity experiment that measures the fraction of light scattered from an incident light beam allows the correlation length amplitude ξ_0 to be determined. Doing both experiments on the same system allows the universal ratio X to be tested in this density-matched system.

The heat capacity has a weak divergence near the critical point that is governed by the critical exponent α, different amplitudes in the one- and two-phase regions, and a critical contribution B_c due to the background heat capacity.[6] Correction to scaling terms extend the theoretical description further from the critical point.[3,6] While a vapor–liquid system measured along the critical isochore would have a weak divergence in the heat capacity at constant volume, a liquid–liquid mixture near its critical consolute point will have the same type of divergence[7] in its heat capacity at constant pressure when measured along a path of constant, critical composition $x = x_c$,

$$C_{px} = (B_{\mathrm{bg}} + B_c) + Et + \frac{A^+}{\alpha}|t|^{-\alpha}(1 + D^+|t|^{\Delta_1} + \cdots) \quad (\text{one phase}), \tag{1a}$$

$$C_{px} = (B_{\mathrm{bg}} + B_c) + Et + \frac{A^-}{\alpha}|t|^{-\alpha}(1 + D^-|t|^{\Delta_1} + \cdots) \quad (\text{two phase}), \tag{1b}$$

where C_{px} is the temperature-dependent heat capacity at constant pressure and at the critical composition, B_{bg} is the background heat capacity far from the critical temperature T_c in the one-phase region, $t = (T - T_c)/T_c$ is the reduced temperature, $A^{\pm}$ is the amplitude of the leading divergence, $D^{\pm}$ is the amplitude of the first correction to scaling term, and Δ_1 is the universal exponent for the correction term. The one- and two-phase amplitudes are denoted by the $(+)$ and $(-)$ superscript, respectively; the background terms and the critical

a)Author to whom correspondence should be addressed; electronic mail: djacobs@wooster.edu

exponents are predicted[6] to be the same above and below the critical point. A linear background term, Et, arises from the regular part of the free energy and hence should also be the same above and below the critical point. The critical exponents α and Δ_1 are predicted[8,9] to be 0.1099 ± 0.0007 and 0.504 ± 0.008, respectively.

The turbidity τ is the inverse of an effective extinction length and is defined by $\tau = (-1/L)\ln(I_t/I_0)$, where L is the length of the scattering medium and I_t is the transmitted, and I_0 the incident, light intensity. The turbidity is caused by light scattering from concentration fluctuations in the fluid mixture near the critical point. By assuming Ornstein–Zernike scattering,[10] which has accurately explained the angular distribution of scattered light near a critical point, an expression for the turbidity can be obtained. A small asymmetry in the forward direction caused Fisher[11] to introduce a critical exponent η whose value[8] is small ($\eta = 2 - \gamma/\nu = 2 - 1.2371/0.630 \sim 0.036$), and results in a negligible effect on the turbidity at the level of this experiment.[12,13] The turbidity can be developed by integrating the light scattered out of the incident beam to give[10]

$$\tau = \tau_0 (1+t) t^{-\gamma} \left[\frac{2a^2 + 2a + 1}{a^3} \ln(1+2a) - \frac{2(1+a)}{a^2} \right], \tag{2}$$

where

$$\tau_0 = \frac{\pi^3}{\lambda_0^4} \left[\frac{\partial n^2}{\partial \phi} \right]^2 k_B T_c \chi_0,$$

$a = 2k_0^2 \xi^2$, $\xi = \xi_0 t^{-\nu}$, $k_0 = 2\pi n/\lambda_0$, $n = 1.4173$ is the refractive index of the mixture,[14] λ_0 is the vacuum wavelength of the light, the turbidity amplitude τ_0 is a quantity dependent on the system, and ν and γ are universal critical exponents. Good data close to T_c are crucial in determining ξ_0 which enters in a complicated fashion through a. The compressibility dominates far from T_c, so the turbidity has a simple power law dependence $\tau = 8\tau_0 t^{-\gamma}/3$ for $T \gg T_c$. Close to T_c, the turbidity varies much more slowly and is a function of both τ_0 and ξ_0: $\tau = [\tau_0/(k_0^2 \xi_0^2)]\ln(2a)$ for $T > T_c$. In experiments very close to T_c, the nonzero value of η becomes important and such a logarithmic dependence is not expected but rather the turbidity goes to a large (but finite) constant, as recently discussed by Ferrell[15] and observed experimentally.[16] The compressibility amplitude χ_0 cannot be determined from τ_0 in this study since measurements of the composition dependence of the refractive index, $\partial n^2/\partial \phi$, are not available.

Some amplitude ratios are predicted to be true universal quantities that should be the same for all systems in a given universality class (three-dimensional Ising for bulk, liquid–liquid mixtures). The ratio of the leading, singular, heat capacity amplitude in the one-phase region to that in the two-phase region is now predicted to be $A^+/A^- = 0.537 \pm 0.019$ by $d = 3$ expansion,[17] 0.530 ± 0.003 by high-temperature series,[8] 0.527 ± 0.037 by ϵ expansion,[17] and 0.56 ± 0.01 by Monte Carlo calculation.[18] One can also relate A^+ to the amplitude ξ_0 of the correlation length in the one-phase region using two-scale-factor universality[8]

$$X = \frac{A^+ \xi_0^3}{k_B},$$

where k_B is Boltzmann's constant. The value of X is predicted from RG[19] to be $X = 0.019\,66 \pm 0.000\,17$ and from high-temperature series[8] to be $0.018\,80 \pm 0.000\,08$.

These predictions have been tested in other liquid–liquid mixtures with mixed results.[1–3] Recent experiments measuring the heat capacity of liquid–liquid mixtures have given A^+/A^- in the range 0.52–0.59;[20–25] a value typically larger than the 0.52 value determined in liquid–vapor systems.[26] Since ξ_0 enters as the cube in X, the error in ξ_0 usually dominates the error in X. A number of values of X, ranging from 0.015 to 0.028, have been determined[5] in a variety of systems. Recent determinations in other liquid–liquid systems have found X to be 0.019 ± 0.003 in triethylamine and water,[24] 0.019 ± 0.004 in triethylamine and heavy water,[22] 0.028 ± 0.007 in 2,6 dimethyl pyridine and water,[27] and 0.020 ± 0.002 in 3-methylpentane and nitroethane[23] while the latest liquid–vapor measurement gives 0.023 ± 0.004 in SF_6.[26]

The values of A^+ and ξ_0 for the succinonitrile–water system reported here have also been determined in earlier measurements, but with large errors. The correlation length amplitude ξ_0 was determined from turbidity measurements[14] to be $\xi_0 = 0.148 \pm 0.070$ nm. The heat capacity was only reported[28] in the one-phase region with an amplitude $A^+ = 0.060 \pm 0.002$ J/(cm^3 K). Our work is a more precise determination of these amplitudes along with measurements of the heat capacity in the two-phase region.

II. EXPERIMENT

A. Fluids

Succinonitrile is a clear, plastic crystal at room temperature. Our sample was from Acros Organics and labled as ''99+%,'' yet was a dark brown resin indicating impurities. After a vacuum distillation, the succinonitrile was clear and a fresh distillation was done for each experimental sample. The water was glass distilled, OmniSolv from EM Science. A critical composition of succinonitrile and water was used in our experiments: 51.9% by mass succinonitrile for both turbidity samples and 51.7% for the heat capacity experiment. These concentrations are consistent with the most recently determined[14] critical concentration of 51.9% by mass (52.3% by volume) succinonitrile, and is the same composition used by other investigators of this system.[29–31] This system exhibits an upper consolute point around 56.1 °C where it has a density[14] of 0.9859 g/cm^3.

B. Heat capacity

The heat capacity of a critical mixture was measured using an adiabatic calorimeter similar to that used previously for studies in triethylamine–water[24] and aniline–cyclohexane.[20] Our calorimeter was used in a ''step'' mode, where a fixed energy was added to the cell and the resulting temperature step was measured. We found this improved the resolution and reproducibility in this system over the scanning mode used initially. Most of the details of

TABLE I. The fluid heat capacity C_p of a critical composition of succinonitrile and water as a function of temperature T. T_c is the critical temperature taken as 328.683 K for run 1, 328.644 for run 2, 328.610 for run 3, and 328.592 K for run 4.

T (K)	C_p (J/cm^3/K)	δC_p (J/cm^3/K)	T (K)	C_p (J/cm^3/K)	δC_p (J/cm^3/K)	T (K)	C_p (J/cm^3/K)	δC_p (J/cm^3/K)	T (K)	C_p (J/cm^3/K)	δC_p (J/cm^3/K)
Run 1											
326.1285	4.238	0.031	328.0518	4.488	0.020	330.3637	3.591	0.023	327.8436	4.492	0.025
326.1575	4.239	0.027	328.0802	4.522	0.024	330.399	3.594	0.023	327.8681	4.470	0.018
326.1864	4.252	0.031	328.1085	4.504	0.021	330.4344	3.580	0.025	327.8965	4.482	0.018
326.2152	4.268	0.031	328.137	4.540	0.017	330.4698	3.585	0.025	327.9248	4.471	0.018
326.2441	4.231	0.029	328.1655	4.528	0.020	330.5051	3.594	0.024	327.9817	4.506	0.011
326.2733	4.265	0.030	328.1933	4.531	0.020	330.5405	3.587	0.024	328.0103	4.516	0.018
326.3023	4.263	0.025	328.221	4.566	0.023	330.5759	3.593	0.025	328.0385	4.526	0.024
326.3313	4.251	0.030	328.2492	4.563	0.027	330.6114	3.589	0.026	328.0667	4.520	0.018
326.3601	4.316	0.037	328.2773	4.614	0.022	330.6468	3.593	0.024	328.0948	4.558	0.016
326.3889	4.253	0.035	328.3052	4.618	0.021	330.6823	3.592	0.025	328.1801	4.562	0.014
326.4178	4.278	0.030	328.3332	4.595	0.022	330.7178	3.586	0.027	328.2081	4.593	0.012
326.4467	4.273	0.023	328.3613	4.614	0.027	330.7534	3.591	0.026	328.236	4.621	0.014
326.4756	4.266	0.022	328.3891	4.686	0.030	330.789	3.577	0.025	328.2637	4.653	0.015
326.5046	4.278	0.023	328.4168	4.684	0.021	330.8245	3.587	0.024	328.2914	4.641	0.011
326.5335	4.288	0.021	328.4444	4.713	0.022	330.8601	3.593	0.024	328.3191	4.674	0.011
326.5624	4.274	0.018	328.472	4.710	0.026	330.8958	3.587	0.024	328.3466	4.695	0.013
326.5914	4.259	0.022	328.4995	4.758	0.027	330.9315	3.579	0.024	328.3741	4.718	0.013
326.6206	4.254	0.021	328.5267	4.779	0.028	330.9671	3.589	0.025	328.4015	4.730	0.016
326.6498	4.274	0.022	328.5536	4.847	0.028	330.003	3.587	0.027	328.4288	4.746	0.021
326.6786	4.323	0.023	328.5805	4.895	0.030	331.0389	3.546	0.027	328.483	4.833	0.018
326.7074	4.305	0.025	328.6072	4.973	0.031	331.0747	3.575	0.026	328.5099	4.861	0.015
326.7362	4.327	0.024	328.6333	5.109	0.030	331.1081	3.565	0.028	328.5366	4.934	0.015
326.765	4.305	0.022	328.6859	4.479	0.025	331.1817	3.591	0.028	328.563	4.981	0.018
326.7938	4.326	0.021	328.7164	3.962	0.020	331.2177	3.566	0.032	328.5891	5.072	0.021
326.8226	4.307	0.018	328.7484	3.891	0.022				328.6147	5.261	0.023
326.8515	4.330	0.016	328.7808	3.844	0.024	Run 2					
326.8797	4.311	0.016	328.8135	3.805	0.024	326.7607	4.311	0.015	328.6675	4.125	0.013
326.908	4.328	0.017	328.95	3.735	0.019	326.7893	4.308	0.017	328.6984	3.976	0.012
326.9366	4.348	0.020	328.9835	3.716	0.021	326.818	4.305	0.019	328.7635	3.879	0.012
326.9652	4.336	0.021	329.0171	3.712	0.020	326.8468	4.309	0.022	328.7958	3.840	0.020
326.9934	4.339	0.021	329.0509	3.731	0.018	326.8755	4.319	0.022	328.8284	3.827	0.017
327.0217	4.336	0.019	329.0847	3.696	0.021	326.9041	4.314	0.020	328.861	3.807	0.012
327.0505	4.330	0.018	329.1185	3.687	0.021	326.9329	4.308	0.024	328.8938	3.791	0.015
327.0794	4.353	0.022	329.1524	3.667	0.021	326.9613	4.317	0.026	328.9268	3.769	0.015
327.1686	4.345	0.018	329.1859	3.678	0.025	326.9897	4.314	0.026	328.9598	3.767	0.017
327.1975	4.364	0.018	329.2195	3.665	0.023	327.0184	4.326	0.020	328.9929	3.753	0.015
327.2262	4.367	0.017	329.2536	3.651	0.021	327.0472	4.300	0.014	329.0262	3.741	0.015
327.255	4.387	0.018	329.2878	3.644	0.019	327.0759	4.349	0.015	329.0593	3.722	0.016
327.2837	4.364	0.019	329.3219	3.678	0.019	327.1046	4.328	0.018	329.0925	3.725	0.021
327.3125	4.383	0.015	329.3561	3.643	0.020	327.1333	4.347	0.019	329.126	3.715	0.022
327.3413	4.394	0.017	329.3904	3.633	0.021	327.162	4.335	0.019	329.1597	3.658	0.018
327.3694	4.415	0.017	329.4249	3.615	0.021	327.1906	4.368	0.019	329.1937	3.658	0.021
327.3975	4.382	0.015	329.4594	3.616	0.020	327.2193	4.338	0.013	329.2276	3.667	0.022
327.4263	4.396	0.013	329.5277	3.607	0.023	327.248	4.365	0.013	329.2621	3.642	0.022
327.455	4.406	0.014	329.5614	3.584	0.024	327.2766	4.361	0.016	329.2966	3.651	0.022
327.4837	4.403	0.014	329.5954	3.621	0.023	327.3052	4.371	0.014	329.3306	3.652	0.018
327.5123	4.419	0.011	329.63	3.611	0.021	327.3339	4.357	0.011	329.3648	3.639	0.019
327.541	4.414	0.013	329.6648	3.589	0.021	327.3625	4.377	0.012	329.399	3.652	0.018
327.5697	4.422	0.014	329.7337	3.602	0.022	327.3911	4.390	0.013	329.4331	3.642	0.017
327.5981	4.443	0.016	329.7685	3.592	0.021	327.4197	4.381	0.014	329.4673	3.642	0.018
327.626	4.399	0.020	329.8035	3.587	0.023	327.4483	4.400	0.012	329.5016	3.634	0.016
327.6542	4.412	0.021	329.8385	3.589	0.023	327.4768	4.388	0.011	329.5359	3.640	0.018
327.683	4.430	0.020	329.8734	3.589	0.025	327.5054	4.392	0.015	329.5702	3.633	0.023
327.7115	4.474	0.019	329.9084	3.596	0.026	327.534	4.414	0.016	329.6047	3.618	0.023
327.7401	4.429	0.017	330.0115	3.582	0.023	327.5625	4.409	0.013	329.6391	3.633	0.019
327.7683	4.418	0.018	330.0466	3.589	0.024	327.591	4.417	0.015	329.6735	3.627	0.021
327.7964	4.453	0.018	330.0817	3.585	0.026	327.6196	4.407	0.014	329.7077	3.581	0.023
327.825	4.462	0.020	330.1169	3.596	0.024	327.6482	4.396	0.012	329.7421	3.604	0.022
327.8535	4.490	0.022	330.152	3.586	0.024	327.6767	4.436	0.015	329.7768	3.601	0.023
327.9107	4.461	0.019	330.1871	3.591	0.021	327.7052	4.427	0.015	329.8115	3.606	0.022
327.9394	4.492	0.019	330.2222	3.615	0.023	327.7337	4.433	0.016	329.8462	3.599	0.023
327.9679	4.502	0.020	330.2575	3.595	0.023	327.7622	4.446	0.020	329.8811	3.591	0.023
327.9961	4.513	0.025	330.2929	3.584	0.020	327.7906	4.447	0.017	329.916	3.585	0.027
328.0238	4.490	0.023	330.3284	3.594	0.022	327.819	4.466	0.015	329.9509	3.586	0.026

TABLE I. (*Continued*.)

T (K)	C_p (J/cm^3/K)	δC_p (J/cm^3/K)	T (K)	C_p (J/cm^3/K)	δC_p (J/cm^3/K)	T (K)	C_p (J/cm^3/K)	δC_p (J/cm^3/K)	T (K)	C_p (J/cm^3/K)	δC_p (J/cm^3/K)
329.9859	3.585	0.022	328.2569	4.664	0.012	Run 4					
330.0209	3.582	0.024	328.2847	4.681	0.012	326.6519	4.325	0.032	328.9971	3.713	0.013
330.0559	3.589	0.024	328.3124	4.692	0.011	326.6806	4.329	0.030	329.0308	3.699	0.014
330.0909	3.572	0.025	328.34	4.731	0.012	326.7093	4.326	0.029	329.1792	3.672	0.014
330.126	3.579	0.024	328.3675	4.747	0.014	326.738	4.340	0.025	329.2133	3.667	0.012
330.1611	3.581	0.021	328.3949	4.786	0.011	326.7667	4.345	0.025	329.2475	3.665	0.012
330.1963	3.575	0.024	328.4221	4.819	0.012	326.7954	4.340	0.024	329.2817	3.662	0.015
330.2314	3.584	0.022	328.4492	4.847	0.015	326.824	4.345	0.024	329.3159	3.655	0.016
330.2666	3.576	0.022	328.4762	4.891	0.016	326.8527	4.351	0.021	329.3502	3.648	0.016
330.3018	3.584	0.023	328.503	4.930	0.012	326.8814	4.347	0.019	329.3845	3.646	0.017
330.3368	3.604	0.022	328.5295	5.007	0.009	326.9101	4.361	0.026	329.4189	3.643	0.014
330.372	3.580	0.023	328.5557	5.112	0.010	326.9387	4.364	0.029	329.4533	3.645	0.015
330.4072	3.578	0.024	328.5813	5.278	0.016	326.9994	4.372	0.020	329.4877	3.645	0.018
330.4424	3.576	0.023	328.635	4.100	0.012	327.028	4.363	0.020	329.5222	3.641	0.015
330.4777	3.572	0.022	328.6664	3.980	0.010	327.0862	4.372	0.028	329.5561	3.637	0.015
330.513	3.588	0.024	328.6983	3.931	0.010	327.2856	4.361	0.014	329.5893	3.635	0.017
330.5483	3.578	0.025	328.7305	3.882	0.010	327.3145	4.371	0.015	329.6233	3.630	0.017
330.5836	3.586	0.027	328.763	3.852	0.009	327.3432	4.378	0.015	329.6579	3.633	0.019
330.6189	3.580	0.026	328.7957	3.837	0.008	327.3721	4.360	0.015	329.6925	3.630	0.019
330.6542	3.575	0.025	328.8279	3.816	0.012	327.4009	4.399	0.017	329.7272	3.627	0.017
			328.8602	3.791	0.013	327.4296	4.385	0.021	329.762	3.622	0.016
Run 3			328.8933	3.804	0.012	327.4584	4.392	0.027	329.7968	3.612	0.017
326.9559	4.388	0.028	328.9264	3.776	0.011	327.4866	4.411	0.023	329.8316	3.608	0.018
326.9843	4.382	0.023	329.0258	3.756	0.010	327.5147	4.406	0.014	329.8659	3.601	0.017
327.0129	4.354	0.026	329.0593	3.745	0.011	327.5435	4.407	0.016	329.9001	3.606	0.015
327.0417	4.345	0.052	329.0929	3.732	0.011	327.5722	4.424	0.023	329.9351	3.600	0.015
327.0703	4.416	0.042	329.1265	3.720	0.012	327.6008	4.429	0.026	329.97	3.599	0.017
327.0989	4.357	0.020	329.1602	3.729	0.014	327.6289	4.421	0.024	330.005	3.594	0.018
327.127	4.390	0.027	329.194	3.706	0.011	327.657	4.457	0.025	330.0401	3.598	0.019
327.1551	4.367	0.025	329.2279	3.707	0.011	327.6856	4.434	0.024	330.0751	3.583	0.021
327.1838	4.395	0.022	329.2618	3.700	0.015	327.7142	4.459	0.016	330.1451	3.598	0.022
327.2124	4.393	0.021	329.2956	3.719	0.013	327.7428	4.459	0.014	330.1782	3.590	0.023
327.241	4.410	0.018	329.3296	3.678	0.009	327.7713	4.467	0.013	330.2106	3.584	0.023
327.2696	4.399	0.018	329.3637	3.700	0.012	327.7999	4.464	0.014	330.2451	3.585	0.020
327.2982	4.410	0.017	329.4321	3.650	0.016	327.8284	4.489	0.014	330.316	3.567	0.025
327.3268	4.427	0.017	329.4663	3.638	0.015	327.8569	4.491	0.010	330.3506	3.571	0.025
327.4127	4.421	0.020	329.5351	3.633	0.021	327.8853	4.501	0.015	330.3854	3.570	0.024
327.4413	4.449	0.016	329.5697	3.627	0.023	327.9137	4.528	0.018	330.421	3.567	0.026
327.4698	4.432	0.012	329.6044	3.619	0.020	327.942	4.530	0.015	330.4565	3.571	0.024
327.4983	4.438	0.015	329.6393	3.616	0.019	327.9703	4.524	0.013	330.4921	3.569	0.023
327.5269	4.432	0.016	329.6741	3.618	0.021	327.9986	4.550	0.015	330.5277	3.578	0.024
327.5554	4.438	0.016	329.7084	3.608	0.022	328.0268	4.553	0.017	330.5634	3.555	0.025
327.584	4.454	0.017	329.742	3.627	0.022	328.055	4.584	0.014	330.5991	3.567	0.028
327.6419	4.460	0.016	329.8116	3.613	0.019	328.0833	4.591	0.015	330.6348	3.558	0.029
327.6704	4.471	0.018	329.8466	3.605	0.020	328.1117	4.581	0.018			
327.6988	4.476	0.013	329.8817	3.597	0.018	328.1398	4.591	0.019			
327.7267	4.476	0.011	329.9168	3.602	0.021	328.1962	4.608	0.014			
327.7547	4.460	0.013	329.9521	3.572	0.023	328.224	4.611	0.015			
327.7832	4.487	0.015	329.9868	3.576	0.023	328.2792	4.633	0.012			
327.8115	4.504	0.015	330.0208	3.578	0.027	328.307	4.665	0.015			
327.8399	4.498	0.015	330.0548	3.584	0.025	328.3348	4.684	0.021			
327.8683	4.509	0.013	330.0894	3.587	0.020	328.3625	4.702	0.021			
327.8967	4.521	0.014	330.1248	3.584	0.026	328.3901	4.728	0.022			
327.925	4.526	0.015	330.1601	3.594	0.028	328.4176	4.771	0.019			
327.9532	4.565	0.014	330.1955	3.581	0.026	328.4443	4.821	0.019			
327.9814	4.526	0.013	330.2309	3.584	0.025	328.4708	4.857	0.020			
328.0075	4.587	0.012	330.2664	3.588	0.024	328.4978	4.882	0.027			
328.0334	4.570	0.014	330.3018	3.581	0.035	328.6671	3.888	0.015			
328.0614	4.614	0.015	330.3373	3.608	0.035	328.6996	3.841	0.018			
328.0894	4.598	0.015	330.3727	3.583	0.024	328.7323	3.807	0.017			
328.1172	4.614	0.015	330.4082	3.582	0.023	328.7653	3.786	0.015			
328.145	4.609	0.014	330.4919	3.590	0.023	328.7985	3.760	0.016			
328.173	4.620	0.011	330.5275	3.588	0.022	328.8317	3.755	0.013			
328.2007	4.648	0.010				328.8979	3.748	0.015			
328.2287	4.648	0.013				328.9305	3.734	0.012			
						328.9634	3.722	0.012			

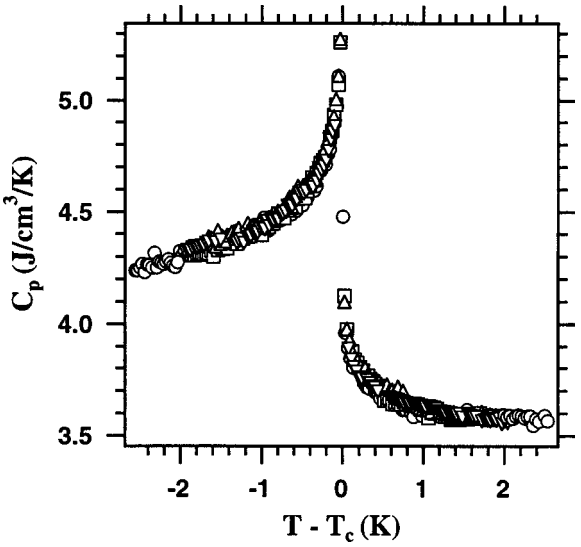

FIG. 1. Heat capacity C_p in succinonitrile–water as a function of temperature T away from the critical temperature T_c given in Table I. All data were taken on the same sample. Symbols for the data are run 1 (circles), run 2 (squares), run 3 (triangles), and run 4 (inverted triangles). The errors in the data are reflected in the reproducibility and are omitted from the plot for clarity.

our calorimeter have been discussed previously and we describe the essential features in the following and refer the interested reader to our earlier work[20,24] for details.

The mixture with a fluid mass of 17.84 g was sealed in a cylindrical, gold plated, copper cell with a Kalrez (DuPont perfluoroelastomer) o ring. The cell is surrounded with a nested set of cylindrical, nickel-plated, copper stages forming a thermostat. A set of actively temperature controlled stages provide an adiabatic environment for the fluids. The outermost stage has an ambient temperature determined by a Lauda RMS-6 bath that circulates water through copper tubing soldered to the outside walls and lid. Some stirring mechanism is essential to achieve thermal equilibrium, especially in the two-phase region.[22–24] Our critical mixture was sloshed by rotating the entire thermostat through a 20° arc with a frequency about 0.6 Hz when current was applied to the cell heater (about 6 min) and then holding the thermostat still while waiting for equilibrium (about 7 min).

The temperature of the stages is determined by thermistors embedded through the lids and into the sidewall of each stage. The cell and stage surrounding it use matched, ''ultrastable'' Thermometrics thermistors while the outer stages use Yellow Springs thermistors. All of the thermistors are wired in series with a 100 kΩ Vishay standard resistor and a 1.5 V battery. The resistance of each thermistor is determined by measuring the voltage across the standard resistor and across each thermistor using a 7 1/2 digit Keithley 2001 multimeter. Each thermistor has been calibrated relative to a Guildline platinum resistance thermometer, which provides an accuracy of 10 mK in absolute temperature.

A computer data acquisition and control software, written in the programming language LABVIEW and using a software PID controlling algorithm, maintains temperature control and records all the stage temperatures with a cycle time of 15 s. A temperature step is achieved by applying 7.5 mW of power to the cell heater for about 6 min, which results in an increase in temperature of the cell and fluids of about 30 mK with a temperature resolution around 0.1 mK.

Four data runs are reported here on a critical composition of succinonitrile and water between 53 and 58 °C. Each data run takes almost three full days and entails over 10 000 sets of stage temperatures, cell temperature, and cell heater voltage. Taking steps allows an average heat capacity to be determined that rounds the anomaly at the critical point. The heat capacities so determined from the four runs are listed in Table I and illustrated in Fig. 1. The errors represent the random fluctuations in the raw data and the propagated error from determining the equilibrium cell temperatures. The critical temperature drifted slightly from one run to the next, which we attribute to small impurities.[32] The effect of minute impurities on the critical point is principally seen as a shift in the critical temperature, with negligible effects on the critical composition, amplitude, or exponents.[32] Table I includes the critical temperature determined for each run.

C. Turbidity

Our light scattering cells were commercial (Spectrocell) made of optical glass with a cylindrical design 22 mm in diameter and a path length of 1.00 and 2.00 cm. Each had a fill tube which was heated and drawn closed to seal the sample. The temperature of the cell was controlled by immersion in a well-stirred, filtered water bath, as described previously.[12,33] The temperature was controlled with a Tronac PTC-41 to give ±0.2 mK maximum excursions over 1 h. The temperature was monitored with a calibrated Thermometrics thermistor whose resistance was measured with a Keithley 2010 digital multimeter to an accuracy of ±10 mK and a precision of ±0.1 mK.

The optical system optimized the precision and accuracy of the light intensity measurements which allowed the turbidity to be determined. The optics has been fully described[12,33] and includes a laser power amplitude controller that provided an incident intensity that varied less than 0.1% long term. The low power laser beam ($\lambda_0 = 632.8$ nm) traveled through the water bath where the cell was oriented with the laser beam along the cell's cylindrical axis. The cell could be moved out of the beam path to determine the absolute turbidity of the fluid sample. The transmitted light intensity was detected by a photodiode with an acceptance angle of 0.3°.

The procedure of taking intensity measurements with the cell in and out of the beam path corrects for reflected and absorbed light from the bath, but not for reflected light from the cell windows. The turbidity due to reflections from the cell windows contributes to a ''background'' turbidity τ_b and is determined by the value of the turbidity well above the critical temperature and is subtracted from the measured turbidity at each temperature to obtain the absolute turbidity τ:

$$\tau = -\frac{1}{L}\ln\left(\frac{I_1}{I_2}\right) - \tau_b, \tag{3}$$

TABLE II. Absolute turbidity τ in the one-phase region of succinonitrile and water as a function of temperature T. T_c is the critical temperature taken as 329.181 K for run 1 (1 cm path length) and 329.195 K for run 2 (2 cm).

T (K)	τ (cm^{-1})	$\delta\tau$ (cm^{-1})	T (K)	τ (cm^{-1})	$\delta\tau$ (cm^{-1})
Run 1			329.1934	0.2585	0.0046
330.9440	0.0046	0.0040	329.1917	0.2955	0.0047
330.4269	0.0046	0.0040	329.1913	0.3025	0.0047
329.7604	0.0058	0.0040	329.1910	0.3265	0.0048
329.7518	0.0073	0.0040	329.1902	0.3135	0.0047
329.7383	0.0088	0.0040	329.1887	0.3825	0.0050
329.7140	0.0103	0.0040	329.1884	0.3235	0.0048
329.6043	0.0093	0.0039	339.1880	0.3475	0.0048
329.5762	0.0136	0.0039	329.1869	0.4215	0.0051
329.5618	0.0150	0.0039	329.1851	0.4815	0.0054
329.5457	0.0163	0.0039	329.1850	0.4165	0.0050
329.5290	0.0149	0.0039	329.1835	0.5645	0.0057
329.5082	0.0179	0.0039	331.3386	0.0041	0.0040
329.5043	0.0179	0.0039	330.4979	0.0040	0.0039
329.4872	0.0208	0.0040	329.4487	0.0211	0.0040
329.4806	0.0236	0.0040	329.4130	0.0279	0.0040
329.4805	0.0236	0.0040	329.3395	0.0396	0.0040
329.4648	0.0221	0.0039	329.2654	0.0736	0.0041
329.4523	0.0192	0.0039	329.2277	0.1262	0.0042
329.4146	0.0263	0.0039	329.2212	0.1422	0.0042
329.4066	0.0265	0.0040	329.2156	0.1568	0.0043
329.3967	0.0275	0.0039	329.2127	0.1681	0.0043
329.3953	0.0293	0.0040	329.2100	0.1797	0.0043
329.3935	0.0292	0.0040	329.2056	0.1966	0.0044
329.3865	0.0308	0.0040	329.1939	0.2924	0.0046
329.3822	0.0310	0.0040	329.1900	0.3528	0.0048
329.3736	0.0365	0.0040	329.1864	0.4394	0.0051
329.3682	0.0335	0.0040	329.1835	0.6215	0.0059
329.3544	0.0322	0.0040	329.1830	0.6996	0.0062
329.3528	0.0371	0.0040	329.1827	0.6598	0.0060
329.3455	0.0398	0.0040	329.1825	0.7081	0.0063
329.3280	0.0468	0.0040	Run 2		
329.3114	0.0496	0.0040	332.0118	0.0007	0.0011
329.2923	0.0618	0.0040	331.1405	0.0022	0.0011
329.2907	0.0541	0.0040	330.3593	0.0030	0.0011
329.2874	0.0606	0.0041	329.6834	0.0100	0.0011
329.2872	0.0540	0.0041	329.5336	0.0154	0.0011
329.2801	0.0648	0.0041	329.3802	0.0314	0.0011
329.2751	0.0738	0.0041	329.3058	0.0565	0.0012
329.2714	0.0693	0.0041	329.2513	0.1065	0.0013
329.2645	0.0739	0.0041	329.2501	0.1043	0.0015
329.2643	0.0714	0.0041	329.2493	0.1058	0.0012
329.2604	0.0721	0.0041	329.2360	0.1394	0.0012
329.2572	0.0815	0.0041	329.2351	0.1441	0.0013
329.2490	0.0875	0.0041	329.2328	0.1461	0.0014
329.2434	0.0935	0.0042	329.2300	0.1529	0.0015
329.2418	0.0925	0.0041	329.2287	0.1583	0.0015
329.2345	0.1055	0.0042	329.2247	0.1718	0.0017
329.2303	0.1195	0.0042	329.2210	0.1920	0.0012
329.2269	0.1205	0.0042	329.2188	0.1981	0.0013
329.2244	0.1275	0.0043	329.2145	0.2313	0.0013
329.2218	0.1305	0.0043	329.2134	0.2367	0.0013
329.2199	0.1405	0.0043	329.2108	0.2582	0.0013
329.2126	0.1635	0.0043	329.2080	0.2818	0.0014
329.2077	0.1745	0.0044	329.2061	0.3100	0.0016
329.2048	0.1935	0.0044	329.2058	0.3139	0.0016
329.2046	0.1975	0.0044	329.2032	0.3573	0.0018
329.1996	0.2175	0.0044	329.2015	0.3906	0.0019
329.1987	0.2355	0.0046	329.1995	0.4531	0.0021
329.1978	0.2265	0.0044	329.1981	0.5046	0.0023
329.1962	0.2415	0.0045	329.1968	0.5736	0.0026
329.1948	0.2475	0.0045	329.1955	0.7199	0.0034

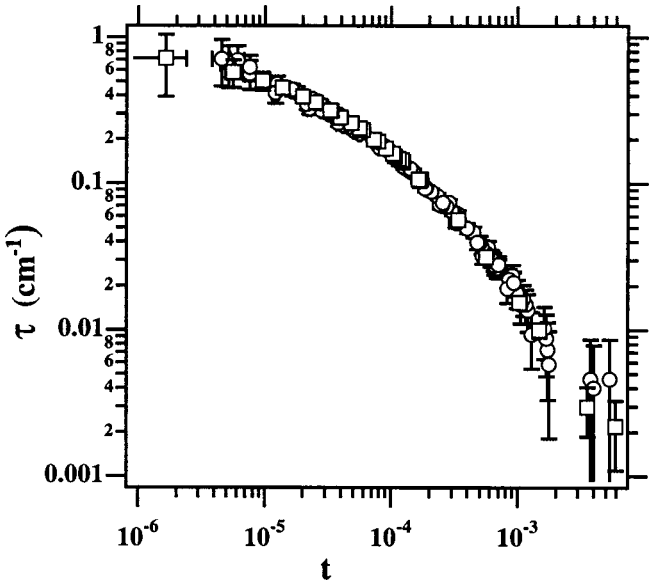

FIG. 2. The absolute turbidity τ in succinonitrile–water as a function of reduced temperature $t=(T-T_c)/T_c$ from Table II. Two different path length cells were used; the 1 cm path length is denoted by a circle while the 2 cm by a square. As t becomes small, the turbidity increases slowly and appears flat in this log–log plot. At larger temperatures, $t>2\times10^{-4}$, the turbidity has a power law dependence on t and follows a straight line with slope $-\gamma$.

where I_1 and I_2 are the ratios of the transmitted to reference intensities with and without the cell in the beam, respectively.

Reproducible data were taken for both the 1 and 2 cm optical path length cells in the one-phase region when $10^{-6}<t<5\times10^{-3}$ $(0.0006°<T-T_c<1.6°)$. The critical temperature was slightly different for each cell, but neither drifted in time. Using two optical path lengths provides a test for multiple scattering when very close to the critical point. In this low light-scattering mixture, no difference in the turbidity was measured between the two cells. The absolute turbidity data are listed in Table II and shown in Fig. 2.

III. ANALYSIS AND INTERPRETATION

A weighted, nonlinear, least-squares routine was used to fit the equations to the data by finding the best set of parameters that minimize[34] the reduced chi-square χ^2/N. In the following, our quoted parameter errors are those given by the program and should be considered the 1σ error.

A. Heat capacity

In analyzing the heat capacity data shown in Table I, we use a simplified version of Eq. (1):

$$C_p=C_{p_0}+Et+\frac{A^+}{\alpha}|t|^{-\alpha}(1+D^+|t|^{\Delta_1}) \quad \text{(one phase)}, \tag{4a}$$

$$C_p=C_{p_0}+Et+\frac{A^-}{\alpha}|t|^{-\alpha}(1+D^-|t|^{\Delta_1}) \quad \text{(two phase)}, \tag{4b}$$

where $t=(T-T_c)/T_c$. In particular, we force equal exponent values above and below the critical point as predicted by theory.[6,7] A smooth, continuous background specific heat near the critical point is expected,[3,6] which means the background amplitudes C_{p_0} and E are the same in the one- and two-phase region. We included a correction-to-scaling term D for some fits with limited success. We simultaneously fit these equations to the one- and two-phase data except the two-phase point in each run closest to T_c, where obvious rounding occurs.

The combined runs were fit over a temperature region within $\pm2°$ of the critical temperature. These 453 data points were well described by six adjustable parameters: C_{p_0}, E, A^+, A^-, T_c, and α. The parameter E should reflect the noncritical fluid behavior and has[35] a small negative value of -0.33 J/(cm^3 K) for the composition used. Allowing E to vary does not improve the fits (see Table III) and thus we fix its value for most fits to the data. Allowing the critical exponent α to vary gives a value of 0.111 ± 0.002, consistent with the theoretical value of 0.11, but doing so substantially increases the errors in the amplitudes. Because of the interdependence of the fitting parameters, it is important to fix critical exponents at their theoretical values so consistent

TABLE III. Parameter values resulting from fitting Eq. (4) to the heat capacity data in Table I. The units on C_{p_0}, E, and A are J/cm^3/K, while D and α are dimensionless, and δT_c is the shift in the critical temperature in mK. χ^2/N is the reduced chi-square. The first set of three fits are to the combined data from the four runs over the temperature region $-2°<T-T_c<2°$ K where correction-to-scaling terms were negligible. The lower three fits are to run 1 over a slightly wider temperature region and include a correction-to-scaling term, but with $A^-\equiv A^+/0.537$ as described in the text. Values in parentheses were fixed; the errors are one standard deviation.

	C_{p_0}	E	A^-	A^+	D	α	δT_c	χ^2/N
Combined								
1c	2.695±0.007	(−0.332)	0.1013±0.0004	0.0543±0.0004	(0)	(0.11)	−0.9±0.3	1.61
2c	2.708±0.028	(−0.332)	0.101±0.003	0.0536±0.0022	(0)	0.111±0.002	−0.8±0.4	1.61
3c	2.675±0.055	−1.3±0.9	0.102±0.006	0.055±0.004	(0)	0.109±0.004	−0.8±0.4	1.61
Run 1								
1e	2.692±0.007	(−0.332)	(Calculated)	0.0542±0.0002	(0)	(0.11)	0	1.40
2e	2.680±0.006	(−0.332)	(Calculated)	0.0532±0.0003	0.48±0.07	(0.11)	−0.6±0.3	1.06
3e	2.59±0.01	−8.1±0.9	(Calculated)	0.0554±0.0004	0.98±0.09	(0.11)	−0.8±0.3	0.62

TABLE IV. Parameter values resulting from fitting Eq. (2) to the combined turbidity data in Table II.

	$\tau_0(\times 10^6\ \mathrm{cm}^{-1})$	ξ_0 (nm)	γ	ν	δT_c (mK)	χ^2/N
$1t$	1.34 ± 0.02	0.168 ± 0.004	(1.237)	(0.630)	1.2 ± 0.4	0.839
$2t$	1.32 ± 0.02	0.168 ± 0.004	(1.2396)	(0.6304)	1.3 ± 0.3	0.838
$3t$	1.2 ± 0.5	0.14 ± 0.02	1.25 ± 0.06	0.65 ± 0.02	0.3 ± 0.4	0.847

amplitudes can be intercompared through universal ratios such as X. Thus, most fits have α fixed. The best is fit $1c$ not only because the reduced chi square is lowest, but the resulting equation is the simplest that fits the combined data. When a correction to scaling term was included, the fit to the combined data over the reduced temperature range did not improve.

Our first run covered the widest temperature range and we used Eq. (4) to fit those data and look for the amplitude D of the correction to simple scaling. To reduce the number of fitting parameters, the fits to run 1 had the same conditions imposed as was done with on the combined data, but also with exponents α and Δ_1 fixed at the theoretical[8] values, $D^+=D^-\equiv D$ (theory predicts[6] the ratio as 0.96 ± 0.25), and the theoretically predicted $A^+/A^-=0.537$. This left five parameters (C_{p_0}, E, A^+, D, and T_c) to describe the 152 points in this run. When D was fixed at zero, the fit (1e) in Table III gave the same parameter values as obtained for the combined data (fit 1c), which indicates the consistency of the data and fitting procedure. The fit to run 1 was improved by including one correction-to-scaling term, as can be seen in fits 2e and 3e each of which had a significantly lower reduced chi-square. The value of D is about what is expected, but its sign is positive while other water based (hydrogen-bonded) liquid–liquid mixtures have found D to be negative either above or below the critical temperature.[24] It should be noted that previous investigations have allowed D^+ and D^- to vary independently, which has resulted in an unexpected switch of signs on either side of the critical temperature. A careful investigation of the amplitudes $D^\pm$ should be done in a system with a larger heat capacity amplitude.

The heat capacity fits given in Table III provide a consistent set of amplitude values when $E=-0.33\ \mathrm{J/(cm^3\,K)}$ and $\alpha=0.11$ are fixed. The background amplitude of Eq. (1) is then: $B_c=-0.90\pm0.03\ \mathrm{J/(cm^3\,K)}$, while $A^+=0.0543\pm0.0004$, $A^-=0.1013\pm0.0004\ \mathrm{J(cm^3\,K)}$, where all the errors are one standard deviation estimates. This value of A^+ is less than the value of $0.060\pm0.002\ \mathrm{J/(cm^3\,K)}$ reported earlier.[28] Our value of the universal ratio $A^+/A^-=0.536\pm0.005$ is consistent with experimental values determined in several liquid–liquid systems recently and with theoretical predictions. Because Knecht[28] did not report any two-phase heat capacity data or results, we cannot compare our ratio to their earlier work.

Another amplitude ratio $R^\pm_{B_{\mathrm{cr}}}=(A^\pm/\alpha)|D^\pm|^{\alpha/\Delta}/B_c$ was introduced by Bervillier[19] and proposed as possibly universal.[36] They predicted[6,19] $R^+_{B_{\mathrm{cr}}}=-0.708\,15$ and $R^-_{B_{\mathrm{cr}}}=-1.334\pm0.044$, which is larger yet consistent with the experimentally[24] determined values of -0.5 and -1.0, respectively. This ratio is fairly insensitive to the value of D and the value we determine for $R^+_{B_{\mathrm{cr}}}=-0.50\pm0.04$ with $R^-_{B_{\mathrm{cr}}}$ determined by our imposed ratio on A for those fits which included D. While the experimental values are consistently less in magnitude than that predicted, one cannot yet conclude either the value or the universality of $R_{B_{\mathrm{cr}}}$.

B. Turbidity

The data shown in Table II were analyzed using a properly weighted least-squares fit where the parameters ξ_0, τ_0, υ, γ, and T_c can all be adjusted in Eq. (2). The resulting values of the parameters are given in Table IV, along with the uncertainties. The data reported in Table II were well explained by an $n=1$ Ising model as shown by the three fits in Table IV.

The first two fits in Table IV use the exponents υ and γ fixed at their theoretical values,[8] which gave equivalent values for the other parameters. The last fit allowed the five parameters τ_0, ξ_0, υ, γ, and T_c to vary freely. When all 122 points were fit by Eq. (2), the values of the exponents were $\upsilon=0.65\pm0.02$ and $\gamma=1.25\pm0.06$, which are close to the known Ising model values.[8] Since the turbidity has a complicated dependence on the critical exponents and because the turbidity is small in this system, it was not possible to accurately determine the critical exponents from this experiment.

Our determination for $\xi_0=0.168\pm0.004\ \mathrm{nm}$ and $\tau_0=(1.34\pm0.02)\times10^{-6}\ \mathrm{cm^{-1}}$ can be compared to the values others have determined for this system. Ataiyan[14] collected and analyzed turbidity data over the region $(0.003°<T-T_c<0.7°)$ and found $\xi_0=0.148\pm0.070\ \mathrm{nm}$ and $\tau_0=(0.8\pm0.1)\times10^{-6}\ \mathrm{cm^{-1}}$, which are smaller than we find. The difference may be due to the additional decade in reduced temperature which we explored. Our reproducibility and precision are reflected in the error estimates on the parameters.

The two-scale-factor universality ratio

$$X=\frac{A^+\xi_0^3}{k_B}$$

can be calculated from our values of $A^+=0.0543\pm0.0004\ \mathrm{J/(cm^3\,K)}$ and $\xi_0=0.168\pm0.004\ \mathrm{nm}$, which gives $X=0.0187\pm0.0013$. This value agrees with other recent experimental determinations and with theoretical predictions.

IV. CONCLUSION

The heat capacity of the liquid–liquid mixture succinonitrile–water has been measured near its upper critical consolute point using an adiabatic calorimeter. The critical exponent α was determined to be 0.111 ± 0.002, consistent with theoretical predictions. When α was fixed at its theoretical value of 0.11, our values of $A^+=0.0543\pm0.0004$ and $A^-=0.1013\pm0.0004\ \mathrm{J/(cm^3\,K)}$, gave a ratio of

A^+/A^- consistent with previous experiments and theory, but the value of A^+ was slightly smaller than previously measured.[28]

From transmitted light intensity data in the one-phase region of the same mixture, the turbidity was well determined in the reduced temperature range $10^{-6}<t<5\times10^{-3}$. Although the data could not accurately determine the critical exponents, when the Ising model values of $\nu=0.63$ and $\gamma=1.237$ were used, the best fit to the data gave amplitudes $\xi_0=0.168\pm0.004\,\mathrm{nm}$ and $\tau_0=(1.34\pm0.02)\times10^{-6}\,\mathrm{cm}^{-1}$. The amplitude ξ_0 of the correlation length is more precisely determined than, yet consistent with, that found previously[14] in this system. Two-scale-factor universality could be directly tested in this system and was found to agree nicely with theoretical predictions and to be consistent with other experimental determinations.

ACKNOWLEDGMENTS

Acknowledgment is made to the donors of The Petroleum Research Fund, administered by the ACS, and to NASA for support of this research. One of us (S.M.M.) acknowledges summer support from NSF REU Grant No. DMR 9619406. D.T.J. thanks the Henry Luce III Fund for Distinguished Scholarship as administered by the College for release time.

[1] J. V. Sengers and J. M. H. Levelt-Sengers, Annu. Rev. Phys. Chem. **37**, 189 (1986).
[2] S. C. Greer and M. R. Moldover, Annu. Rev. Phys. Chem. **32**, 233 (1981).
[3] A. Kumar, H. R. Krishnamurthy, and E. S. R. Gopal, Phys. Rep. **98**, 57 (1983).
[4] M. E. Fisher and J.-H. Chen, J. Phys. (Paris) **46**, 1645 (1985).
[5] D. Beysens, A. Bourgou, and P. Calmettes, Phys. Rev. A **26**, 3589 (1982).
[6] C. Bagnuls, C. Bervillier, D. I. Meiron, and B. G. Nickel, Phys. Rev. B **35**, 3585 (1987).
[7] M. A. Anisimov, *Critical Phenomena in Liquids and Liquid Crystals* (Gordon and Breach, Philadelphia, 1991).
[8] M. Campostrini, A. Pelissetto, P. Rossi, and E. Vicari, Phys. Rev. E **60**, 3526 (1999).
[9] P. Butera and M. Comi, Phys. Rev. B **58**, 11552 (1998).
[10] V. G. Puglielli and N. C. Ford, Jr., Phys. Rev. Lett. **25**, 143 (1970).
[11] M. E. Fisher, J. Math. Phys. **5**, 944 (1964).
[12] D. T. Jacobs, Phys. Rev. A **33**, 2605 (1986).
[13] C. Houessou, P. Guenoun, R. Gastaud, F. Perrot, and D. Beysens, Phys. Rev. A **32**, 1818 (1985).
[14] J. Ataiyan, H. Kreuser, L. Belkoura, G. Quirbach, F. J. Wirtz, and D. Woermann, Z. Phys. Chem. (Munich) **177**, 173 (1992).
[15] R. A. Ferrell, Physica A **177**, 201 (1991).
[16] D. T. Jacobs, S. M. Y. Lau, A. Mukherjee, and C. A. Williams, Int. J. Thermophys. **20**, 877 (1999).
[17] R. Guida and J. Zinn-Justin, J. Phys. A **31**, 8103 (1998).
[18] M. Hasenbusch and K. Pinn, J. Phys. A **31**, 6157 (1998).
[19] C. Bervillier and C. Godrèche, Phys. Rev. B **21**, 5427 (1980).
[20] P. F. Rebillot and D. T. Jacobs, J. Chem. Phys. **109**, 4009 (1998).
[21] L. V. Entov, V. A. Levchenko, and V. P. Voronov, Int. J. Thermophys. **14**, 221 (1993).
[22] E. Bloemen, J. Thoen, and W. Van Dael, J. Chem. Phys. **73**, 4628 (1980).
[23] G. Sanchez, M. Meichle, and C. W. Garland, Phys. Rev. A **28**, 1647 (1983).
[24] A. C. Flewelling, R. J. DeFonseka, N. Khaleeli, J. Partee, and D. T. Jacobs, J. Chem. Phys. **104**, 8048 (1996).
[25] J. Thoen, J. Hamelin, and T. K. Bose, Phys. Rev. E **53**, 6264 (1996).
[26] A. Haupt and J. Straub, Phys. Rev. E **59**, 1795 (1999).
[27] M. Jungk, L. Belkoura, D. Woermann, and U. Wurz, Ber. Bunsenges. Phys. Chem. **91**, 507 (1987).
[28] B. Knecht and D. Woermann, Z. Phys. Chem. (Munich) **191**, 265 (1995).
[29] J. Ataiyan and D. Woermann, Z. Phys. Chem. (Munich) **189**, 139 (1995).
[30] L. H. Ng and D. R. Sadoway, Can. J. Chem. **66**, 2428 (1988).
[31] J. E. Smith, Jr., D. O. Frazier, and W. F. Kaukler, Scr. Metall. **18**, 677 (1984).
[32] J. L. Tveekrem and D. T. Jacobs, Phys. Rev. A **27**, 2773 (1983).
[33] S. G. Stafford, A. C. Ploplis, and D. T. Jacobs, Macromolecules **23**, 470 (1990); L. W. DaMore and D. T. Jacobs, J. Chem. Phys. **97**, 464 (1992).
[34] P. R. Bevington, *Data Reduction and Error Analysis for the Physical Sciences* (McGraw–Hill, New York, 1969).
[35] *Recommended Reference Materials for the Realization of Physicochemical Properties*, edited by K. N. Marsh (Blackwell Scientific, Oxford, 1987); C. A. Wulff and E. F. Westrum, Jr., J. Phys. Chem. **67**, 2376 (1963).
[36] C. Bagnuls and C. Bervillier, Phys. Lett. A **195**, 163 (1994).